Egypt. J. Chem. **Vol. 67**, No. 5 pp. 23 - 42 (2024)

Egyptian Journal of Chemistry

http://ejchem.journals.ekb.eg/

Synthesis and Characterization of Chitosan Nanoparticles from some Crustacean Wastes

Abdelrahman S. Talab[a],*, Ahmed M.S. Hussein[b], Mohie M. Kamil[b], Sayed Mostafa[b], Nefisa A. Hegazy[b] and Khaled F. Mahmoud[b]

[1]National Institute of Oceanography and Fisheries, Egypt.
[2]Food Technology Department, Food Industries and Nutrition Research Institute, National Research Centre, 12622 Dokki, Cairo, Egypt

Abstract

Chitosan (CS) and chitosan nanoparticles (CS/NPs) were prepared from shrimp and crab wastes and they were characterized using spectral analysis, Fourier transforms infrared spectroscopy (FTIR), Scanning electron microscopy (SEM) and Energy Dispersive analysis of X-Ray and Spectroscopy (EDAX) analysis. Also, functional and physicochemical properties of the extracted chitosan and chitosan nanoparticles were analysed. The morphological properties of chitosan and its nanoparticles revealed a smooth surface and fibrous structures with pores. Crab chitosan and its nanoparticles had the highest values of moisture (6.13 and 6.20%) and ash contents (2.60 and 2.90%), respectively. While the highest value of nitrogen (8.50%) was found in commercial chitosan. The highest extraction yield (16.33%) was recorded for crab chitosan compared with (15.35%) for shrimp chitosan. Water binding capacity was higher (780-782%) in shrimp chitosan and its nanoparticles, whereas commercial chitosan and its nanoparticles recorded the highest values (539-539%) fat binding capacity. On the other hand, shrimp chitosan and its nano-type recorded the highest degrees of deacetylation values 92% and 90%, respectively. The solubility was proportional to the degree of deacetylation. The results revealed that chitosan nanoparticles process improved the physicochemical, functional, and morphological characteristics of the extracted chitosan.

Keywords: Chitosan nanoparticles, FTIR, SEM, EDAX.

1. Introduction

Crustaceans traded annually, 6 to 8 million tons of valuable shrimp, lobster and/or crab shells waste are produced worldwide **[1].** The last numbers reported indicate that, from the fish caught, around 70 % is industrially processed **[2]** thus resulting in the production of large amounts (approximately 20–80 %) of wastes **[3].**

Seafood, by its turn being the most traded food commodity worldwide **[4],** reached a global market of USD 164.1 billion in 2018, and is projected to reach USD 194 billion by 2027 **[5].** From the seafood traded annually, 6 to 8 million tons of crab, shrimp and lobster shells waste are globally produced **[6].** Contrarily to what happens in developing countries, where the shells waste is simply dumped in landfill, in the developed countries, their disposal can be costly **[6].** Crustacean shells are composed mainly of 20–30 % of proteins, 30–40 % of calcium carbonate ($CaCO_3$), 20–30 % of chitin and a smallest amount of astaxanthin **[7].** There is a high commercial value for these natural compounds, namely considering their main uses. Shrimp waste, which is rich in chitin, proteins, lipids, pigments and flavor compounds, has

*Corresponding author e-mail: abdelrahman_saidh@yahoo.com
Receive Date: 08 August 2023, Revise Date: 02 November 2023, Accept Date: 26 November 2023
DOI: 10.21608/EJCHEM.2023.228113.8401

potential commercial value in the food industry **[4]**.

Chitosan nanoparticles (CS/NPs) can be used for various applications because of their unique properties like, biodegradability, high permeability, non-toxicity to human and cost effectiveness. CS at nanometer scale presents antimicrobial properties mainly due to its large surface area. This fact has promoted the study of CS/NPs with the purpose of using them as new antimicrobial agents. The effect of CS/NPs against several types of bacteria has been extensively studied **[8-9]**. The antifungal activity of CS/NPs against fungi, *Macrophomin-aphaseolina* and *Pyricularia-grisea*, *Alternariasolani*, *F. oxysporum* has been reported by **[10-11]**, respectively.

Therefore, the main objective of this work was to prepare chitosan and chitosan nanoparticles from shrimp and crab wastes and compared them with commercial chitosan. This objective will be achieve through comparing the characteristics of their physicochemical properties using X-ray, FTIR, and EDEX analysis.

2. Materials and methods

2.1. Materials

Shrimp shells and crab exoskeletons were obtained from fish local market and they were extracted according to the method explained by **Toan [12]**

2.2. Methods

2.2.1. Chitosan preparation

Firstly shrimp and crab wastes were suspended in 4 % HCl at room temperature in the ratio of 1:14 (w/v) for 36 h. Deproteinization of shells was done by treating the demineralized shells with 5 % NaOH at 90°C for 24 h with a solvent to solid ratio of 12:1 (v/w). After the incubation time the shells were washed to neutrality in running tap water and sun dried. The product obtained was chitin which was deacetylatiedby employing 70 % NaOH solution with a solid to solvent ratio of 1:14 (w/v) and incubated at room temperature for 72 h and then, the residues were washed with running tap water to neutrality and rinsed with deionized water, then filtered, sun dried and finely grinded to obtained chitosan **[13]**.

2.2.2. Preparation of chitosan nanoparticles

Conventional particle size reduction techniques such as ball milling process (Ball milling Model: PQ-N2 Planetary Ball Mill, Gear Drive 4- station – planetary Ball mill, 220 v) was used for preparation of chitosan nanoparticles (CS/NPs) according to **Joni, *et al*., [14] and Inkyo, *et al*., [15]** as follows: 25 g weight of chitosan powder was ball milled in a 200 ml agate vessel with 130 numbers of zirconia beads in range from 0.5 to 1.5 mm diameter (75 beads 0.5 mm diameter, 30 beads 1.0 mm diameter and 25 beads 1.5 mm diameter) and milling at 4000 rpm in a high energy planetary ball mill was performed . Different samples were prepared by varying the milling duration, and then the dried chitosan powder was pulverized for 90 min to obtain fine powder. A Ball milling process was used as a dispersing agent to prevent particles agglomeration.

2.2.3. Milling Procedure

The dried chitosan was pulverized by ball mill to obtain fine powder. The obtained powder was selected to obtain more uniform micron size (around 37 μm) by using sieves with mesh 400 and subjected to beads

milling process according to the method of **Ibrahim*, et al*., [16].**

The bead mill consists of 200 ml vessel, a pump and a mixing tank. The vessel was filled with beads up to 70% capacity. The slurry was prepared by mixing the chitosan powder and distilled water. The mixed chitosan was stirred using magnetic stirrer for 30 minutes before beads milling. The PEG 400 (Polyethylene glycol) dispersing agent was added after the mixing time of 15 minutes. The slurry of the chitosan was added into the vessel which contained zirconia beads and impeller operated at a speed of 4000 rpm. The beads were agitated in the lower portion of the vessel (dispersing section) to break up the aggregate to avoid agglomeration of chitosan nanoparticles in the suspension. After dispersion, the suspension was placed from the dispersing section to separation region where centrifugal force was used to separate the zirconia beads from the particle suspension. The chitosan particle suspension was then recycled back to the dispersing section. In order to keep the temperature of the system constant (25°C), the vessel was supported by a water jacket system and was completely sealed. The water-suspended chitosan particles with weight fractions of 0.1 wt. %, milling time 90 minutes and addition acetic acid solution (1%, v/v) after milling to promote the positive surface charge were used for optimal technical conditions for beads milling. After milling process, chitosan was freeze-dried (LABCONCO, Kansas City, USA) at 50 °C and 0.014 mbar for 2 days to reach moisture content 4 %.

2.3. Analysis

Moisture and ash contents of obtained chitosan and chitosan nanoparticles were determined according to the **AOAC [17].** Yield was determined according to **Mohanasrinivasan*, et al*., [18].** Water and fat binding capacity were measured according to **Wang and Kinsella [19].**

Fourier Transform Infrared (FTIR) Spectroscopy: The samples of prepared chitosan and chitosan nanoparticles were characterized in KBr pellets by using an infrared spectrophotometer model (4100 Jasco, Japan) in the range of 400-4000 cm^{-1}.

Degree of deacetylation (DD): FTIR instrument was used for the determination of DD of the three types of chitosan. The percentage of the acetylated amine group was determined by the following formula: DD (%) = 100 - [(A1629.85cm-1- A3450.65 cm-1)/1.33× 100]. **Struszczyk [20].**

Scanning electron microscopy (SEM) having a magnification range of 5,000 and accelerating voltage 20 kV were used for characterization of prepared chitosan and chitosan nanoparticles.

Elements contents of chitosan samples were evaluated by using Energy Dispersive analysis of X-Ray Spectroscopy (JED-2300 analysis station, Joel). EDAX (Energy Dispersive analysis of X-Ray Spectroscopy) analysis used for chitosan characterization by (JED-2300 analysis station, Joel).

Results and Discussion

Chitosan and chitosan nanoparticles were extracted from shrimp and crab wastes and compared with commercial chitosan as shown in **Table (1).** Results showed that, the yield of chitosan from shrimp and crab waste was accepted, where it reached to 15.35 and 16.33%, respectively. The differences in chitosan extraction yield can be attributed to the origins of the polymer

[21]. Moisture and nitrogen contents of the different types of chitosan ranged between (4.10–6.20%) and (7.32-8.50%), respectively.

Table (1). Functional and physicochemical properties of the three chitosan types (commercial, shrimp and crab).

Properties (%)	T1	T2	T3	T4	T5	T6
Yield	**-**	**-**	**15.35**	**-**	**16.33**	**-**
Moisture	**4.10**	**4.50**	**5.11**	**5.50**	**6.13**	**6.20**
Nitrogen	**8.50**	**8.12**	**7.32**	**7.32**	**8.16**	**8.16**
Ash	**1.20**	**1.13**	**1.80**	**1.85**	**2.60**	**2.90**
WBC	**665**	**670**	**780**	**782**	**745**	**750**
FBC	**539**	**539**	**520**	**515**	**525**	**530**
DD	**85**	**83**	**92**	**90**	**86**	**88**

Where, T1: commercial chitosan; **T2:** commercial chitosan nanoparticles; **T3:** shrimp chitosan; **T4:** shrimp chitosan nanoparticles; **T5:** crab chitosan; **T6:** crab chitosan nanoparticles; **WBC:** Water binding capacity; **FBC:** Fat binding capacity; **DD:** Degree of deacetylation.

The moisture content of chitosan is largely related to the species of polymer and the lower moisture content of chitosan, the better its quality and shelf stability **[21-23]**.

Ash is an important indicator to evaluate the purity of chitosan and the efficiency of the demineralization process **[24]** and the ash content of chitosan is primarily depends on the starting material and its composition **[25]**. Higher amounts of ash were found in crab chitosan and its nanoparticle (2.60 and 2.90 %) compared to commercial chitosan (1.20%) or shrimp chitosan (1.80%). Water binding capacity and fat binding capacity mainly depend on the demineralization and deproteinization steps **[226-27]**.

Water binding capacity (WBC) and fat binding capacity (FBC) is one of the most important characters that affect on texture of food product. WBC was higher in shrimp chitosan (780%) and crab chitosan (745%) compared to commercial chitosan (665%). It was noticed that, there were no significant differences in FBC of commercial chitosan, shrimp chitosan and crab chitosan, where they ranged between 520-539%. On the other hand, the degree of deacetylation is a vital parameter because it influences the physical, chemical, mechanical, and biological properties of the biopolymer **[28]**.

Our results showed that, the degree of deacetylation (DD) was accepted in chitosan of shrimp or crap compared to commercial chitosan, where they ranged between 85-92%. The differences in the degree of deacetylation (DD) of chitosan can be attributed to the extraction process, as well as the initial source material **[29]**. Similar results were reported by **[30-33]**.

Characterization of chitosan samples

Fourier Transform Infrared (FTIR) Spectroscopy Functional groups of both commercial, shrimp and crab shells chitosan and their nanoparticles samples were identified by Fourier transform infrared (FTIR) spectroscopy.

The FTIR spectra obtained of chitosan and chitosan nanoparticles samples are

shown in **Fig. (1).** On the other hand, **Table (2)** summarized the characteristic bands of commercial, shrimp and crab chitosan and their nanoparticles samples.

The FTIR peaks for commercial chitosan (T1) and commercial chitosan nanoparticles (T2) were observed at 3282.69 cm^{-1} and 3180.95-3103.28 cm^{-1} (NH and O-H stretching vibrations), 2919.08-2871.26 cm^{-1} and 2971.52-2598.28 cm $^{-1}$ (axial stretching of C-H in the polymer chain), 1643.52-1555.82 cm^{-1} and 1628.61-1548.12 cm^{-1} (amide I vibration modes), 1417.62-1376.29 cm^{-1} and 1461.15-1388.98 cm^{-1} (N-H straining vibrations of NH_2 groups), 1314.93 cm^{-1} and 1295.62 cm-1 (CH_2 deformation vibrations), 1149.58 cm^{-1} and 1136.60 cm^{-1} (symmetrical angular deformation of CH_3 in $NHCOCH_3$ groups), 1061.55 cm^{-1} and 1035.39 cm^{-1} (amide III vibration modes), 897.37 cm^{-1} and 908.85 cm^{-1} (C-O-C bridge), 709.73-414.16 cm^{-1} and 661.11-430.98 cm^{-1} (C-O stretching vibration of alcohol groups), respectively.

The FTIR peaks for shrimp chitosan (T3) and shrimp chitosan nanoparticles (T4) were observed at 3263.213093.76 cm^{-1} and 3816.95-3103.67 cm^{-1} (N-H and O-H stretching vibrations), 2919.35-2851.05 cm-1 and2942.78-2239.16 cm^{-1} (axial stretching of C-H in the polymer chain), 1627.21-1558.30 cm^{-1} and 16.29.00-1549.78 cm^{-1} (amide I vibration modes), 1480.09-1328.63cm-1 and 1461.39-1389.18 cm-1 (N-H straining vibrations of NH_2 groups), 1203.91 cm^{-1} and 1295.69 cm^{-1} (CH_2 deformation vibrations), 1154.24 cm^{-1} and 1137.23 cm^{-1} (symmetrical angular deformation of CH_3 in $NHCOCH_3$ groups), 1067.89-1025.32 cm^{-1} and 1049.44-1034.74 cm^{-1} (amide III vibration modes), 952.70 cm^{-1} and 909.17 cm^{-1} (C-O-C bridge), 654.45-418.20 cm^{-1} and 661.89-432.29 cm^{1} (C-O stretching vibration of alcohol groups), respectively.

The FTIR peaks for crab chitosan (T5) and crab chitosan nanoparticles (T6) were observed at 3859.41-3263.14 cm^{-1} and 3861.13-3283.31 cm^{-1} (N-H and O-H stretching vibrations), 2921.73-2852.21 cm^{-1} and 2872.99-2326.58 cm^{-1} (axial stretching of C-H in the polymer chain), 1642.64-1551.73 cm^{-1} and 1810.28-1550.93 cm^{-1} (amide I vibration modes), 1410.03-1326.68 cm^{-1} and 1424.99 cm^{-1} (N-H straining vibrations of NH_2 groups), 1204.70 cm^{-1} and 1315.57 cm^{-1} (CH_2 deformation vibrations), 1154.07 cm^{-1} and 1150.54 cm^{-1} (symmetrical angular deformation of CH_3 in $NHCOCH_3$ groups), 1067.91-10.28.20 cm^{-1} and 1060.90-1024.37 cm^{-1} (amide III vibration modes), 952.62-711.35 cm^{-1} and 898.42-798.05 cm^{-1} (C-O-C bridge), 637.89-418.89 cm^{-1} and 591.85-418.58 cm^{-1} (C-O stretching vibration of alcohol groups), respectively.

The obtained results showed that, all samples of chitosan and its nanoparticles had high concentration and not detected any contaminant. Similar results were reported by **[33-36]**.

Fig. (2a-f) showed the characterization of chitosan and chitosan nanoparticles samples by X-ray diffraction (XRD) technique.

The XRD studies of commercial chitosan showed a sharper peak at 40° (1187.91 counts/s) and a maximum peak at 30° (2308.63 counts/s), while, commercial chitosan nanoparticles revealed stronger peaks at 10° (82628.7 counts/s) and a maximum reflection at 21.675° (98817.5 counts/s).

Table (2). The FTIR bands (cm^{-1}) of commercial, shrimp and crab shells chitosan and its nanoparticle samples.

Functional groups and vibration modes	T1	T2	T3	T4	T5	T6
Stretching vibrations of hydroxyl groups (OH) Asymmetric/symmetric stretching of the amine bonds (NH_2)	3282.69	3180.95 3103.28	3263.21 3093.76	3816.95 3746.31 3180.19 3103.67	3859.41 3642.43 3263.14	3861.13 3283.31
C-H aliphatic stretching vibration (CH2)	2919.08 2871.26	2971.52 2598.28	2919.35 2851.05	2942.78 2239.16	2921.73 2852.21	2872.99 2326.58
Amide frequencies of C=O bond stretching of amide I	1643.52 1555.82	1628.61 1548.12	1627.21 1558.30	1629.00 1549.78	1642.64 1551.73	1810.28 1550.93
N-H bending vibrations of NH_2 groups of the amide II	1417.62 1376.29	1461.15 1388.98	1480.09 1328.63	1461.39 1389.18	1410.03 1326.68	1424.99
CH_2 deformation vibrations in the CH_2OH groups	1314.93	1295.62	1203.91	1295.69	1204.70	1315.57
Symmetrical angular deformation of CH_3 in $NHCOCH_3$ groups	1149.58	1136.60	1154.24	1137.23	1154.07	1199.02 1150.54
C-N stretching vibrations of amide III	1061.55 1024.12	1035.39	1067.89 1025.32	1049.44 1034.74	1067.91 1028.20	1060.90 1024.37
Symmetric/asymmetric stretching signals of the C- O-C bridge (glycolsidic linkage)	897.37	908.85	952.70 872.13	909.17	952.62 711.35	898.42 798.05
C-O stretching vibration in secondary and primary OH groups	709.73 414.16	661.11 430.98	654.45 418.20	661.93 432.29	637.89 418.89	591.85 418.58

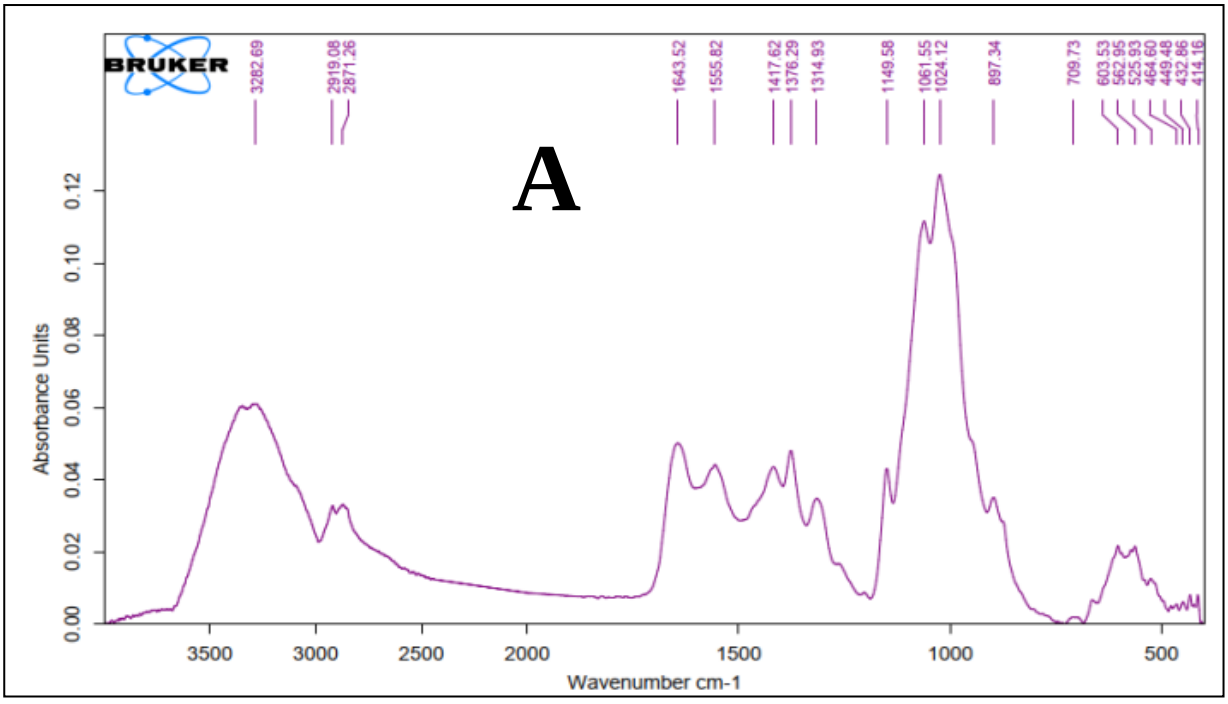

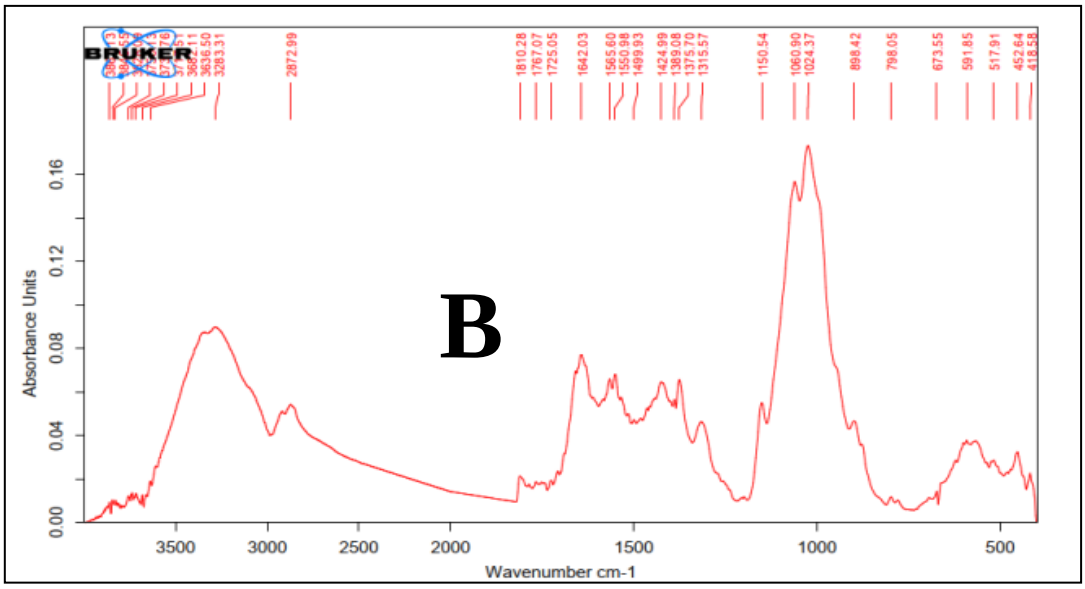
BRUKER
3636.50
3283.31
2887.99
1810.28
1767.07
1725.05
1642.03
1565.60
1550.98
1499.93
1424.99
1389.08
1375.70
1315.57
1150.54
1060.90
1024.37
898.42
798.05
673.55
591.85
517.91
452.64
418.58
B
Absorbance Units
0.00
0.04
0.08
0.12
0.16
3500
3000
2500
2000
1500
1000
500
Wavenumber cm-1

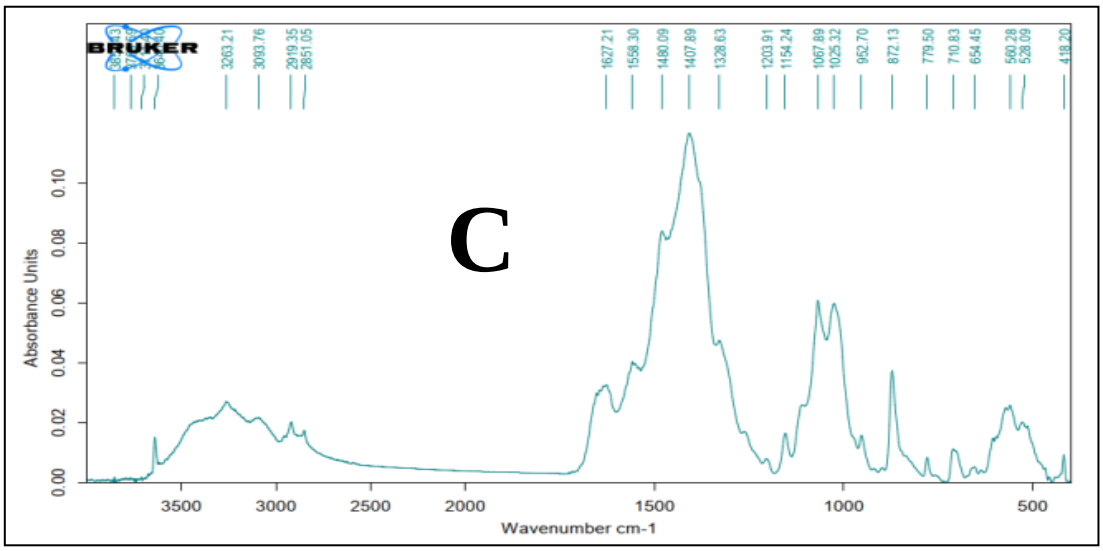
BRUKER
3263.21
3093.76
2919.35
2851.05
1627.21
1558.30
1480.09
1407.89
1328.63
1203.91
1154.24
1067.89
1025.32
952.70
872.13
779.50
710.83
654.45
560.28
528.09
418.20
C
Absorbance Units
0.00
0.02
0.04
0.06
0.08
0.10
3500
3000
2500
2000
1500
1000
500
Wavenumber cm-1

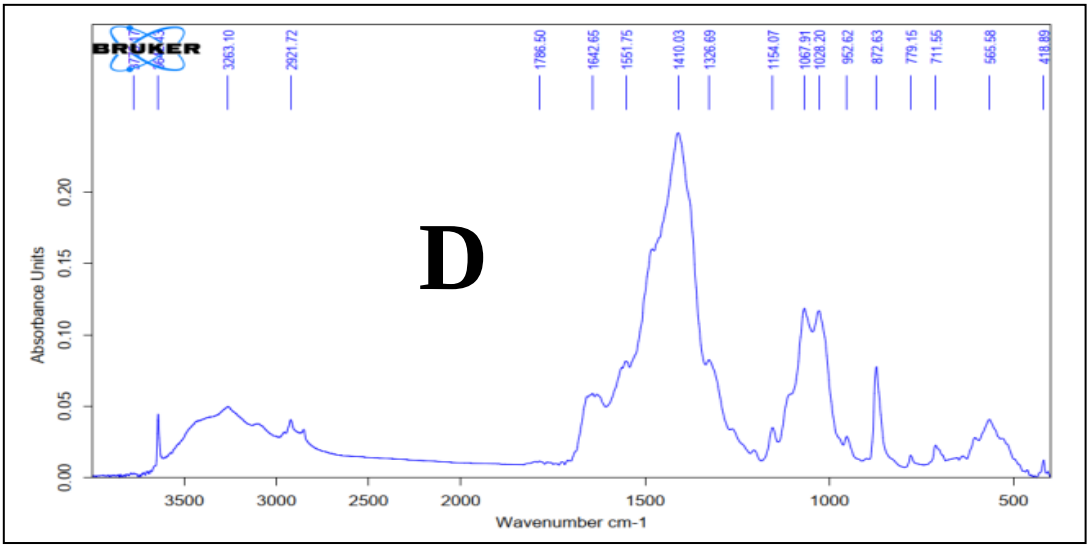
BRUKER
3263.10
2921.72
1786.50
1642.65
1551.75
1410.03
1326.69
1154.07
1067.91
1028.20
952.62
872.63
779.15
711.55
565.58
418.89
D
Absorbance Units
0.00
0.05
0.10
0.15
0.20
3500
3000
2500
2000
1500
1000
500
Wavenumber cm-1

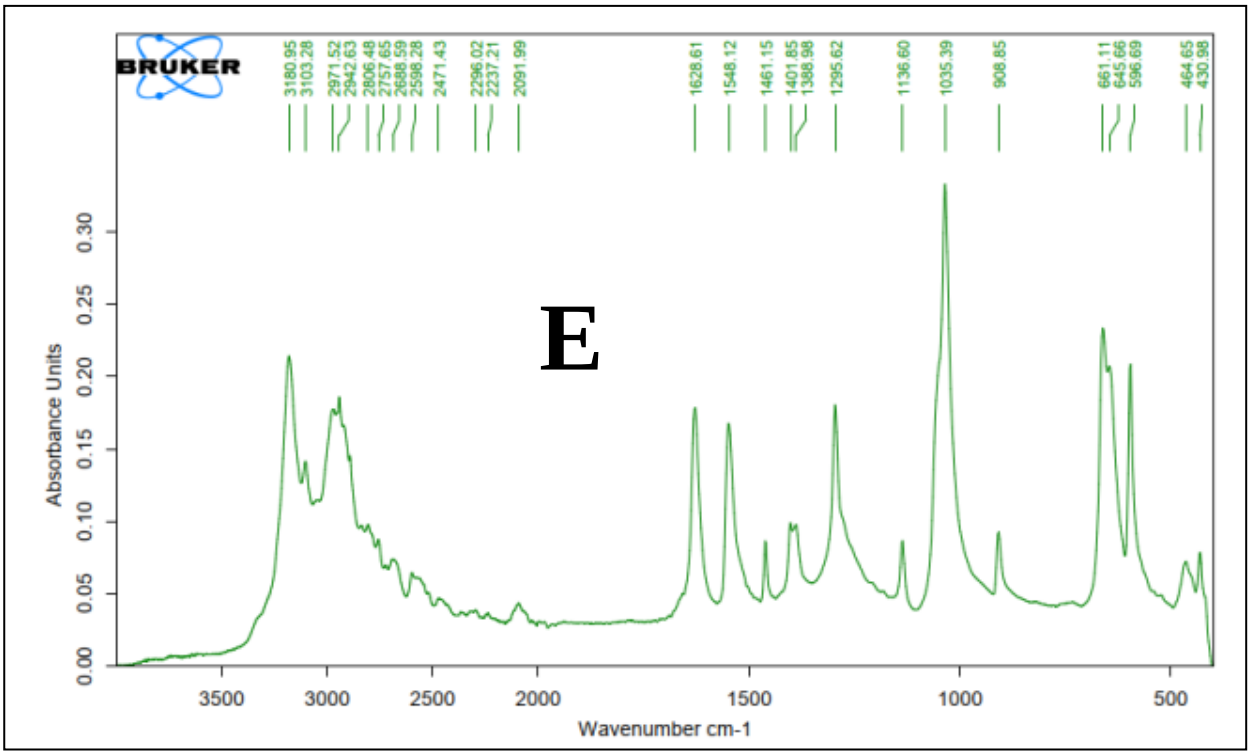

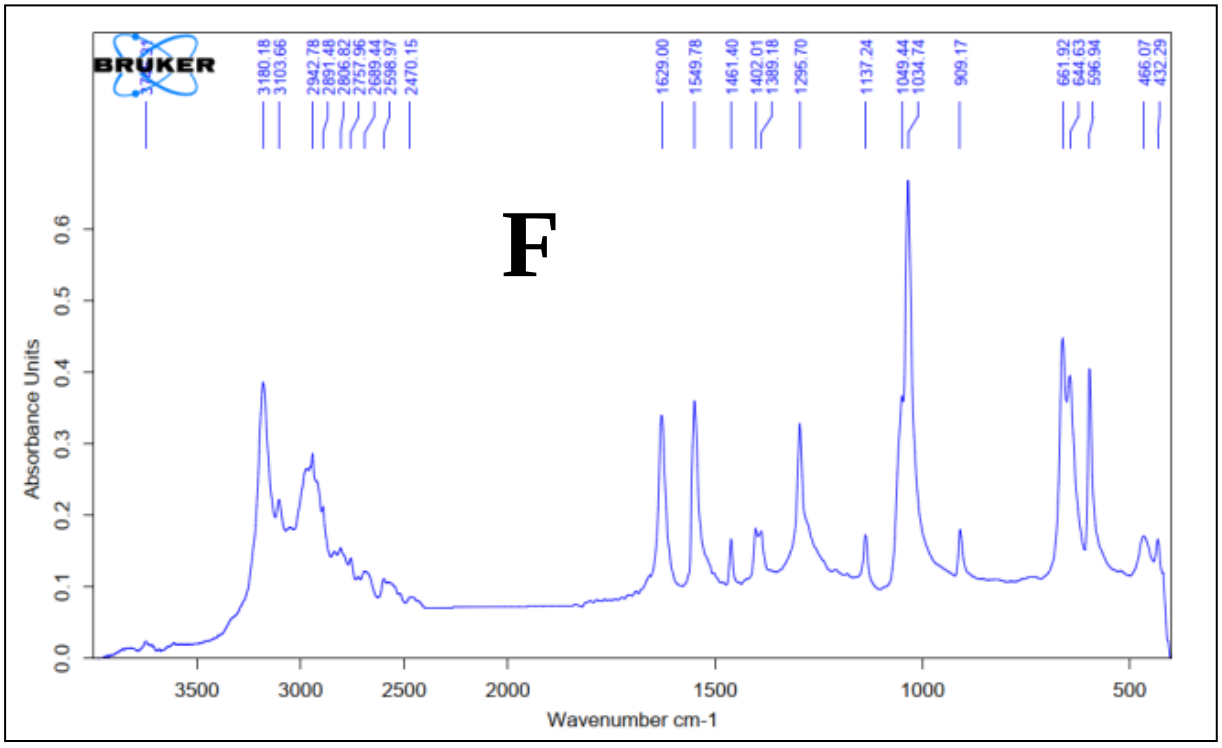

Fig. (1). FTIR of **(A)** commercial chitosan, **(B)** commercial chitosan nano-particles, **(C).** FTIR of shrimp chitosan, **(D)** shrimp chitosan nanoparticles, **(E)** crab chitosan and **(F)** crab chitosan nanoparticles.

X-ray Diffraction (XRD)

Fig. (2a-f) showed the characterization of chitosan and chitosan nanoparticles samples by X-ray Diffraction (XRD) technique.

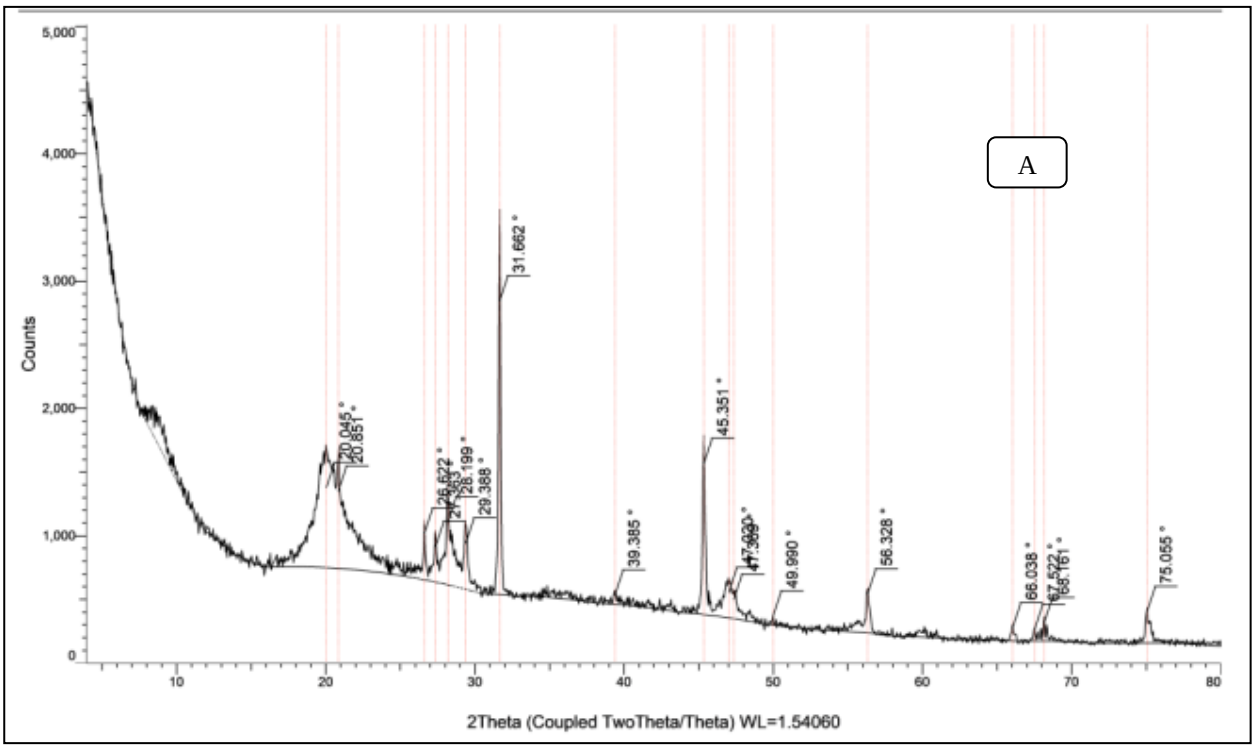

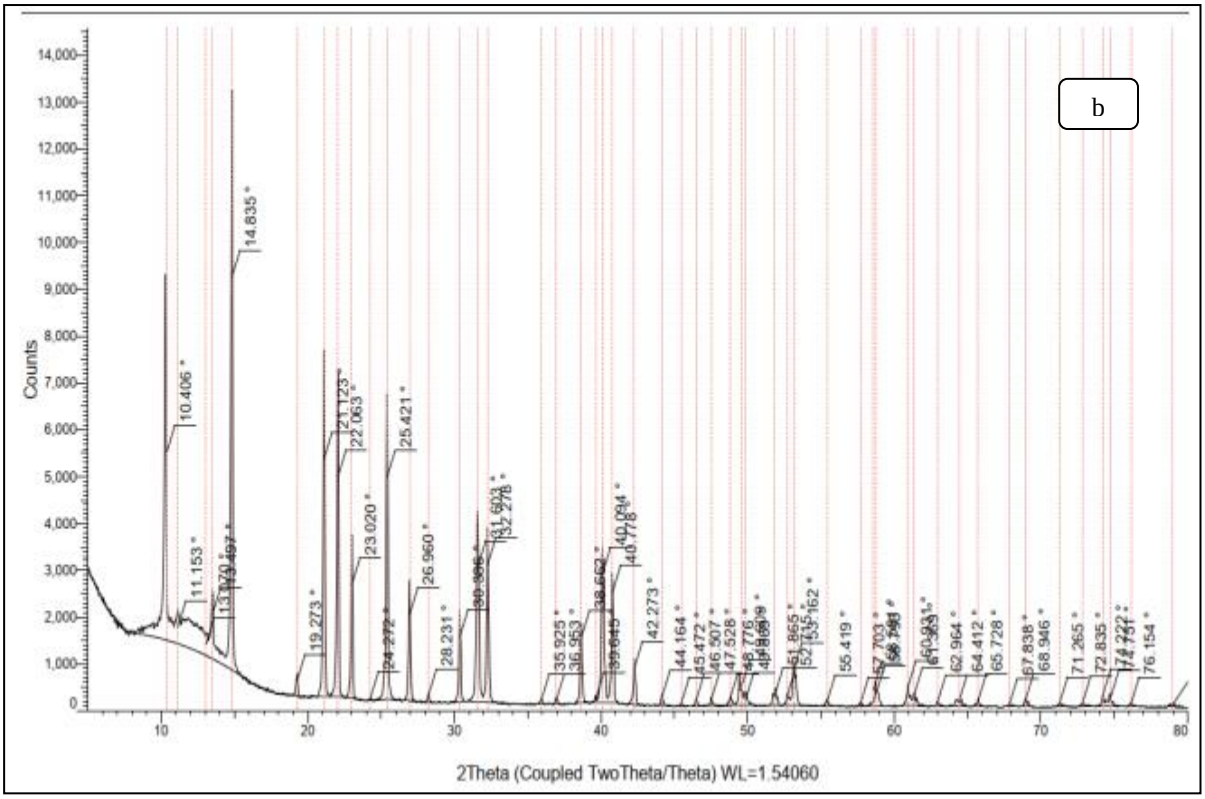

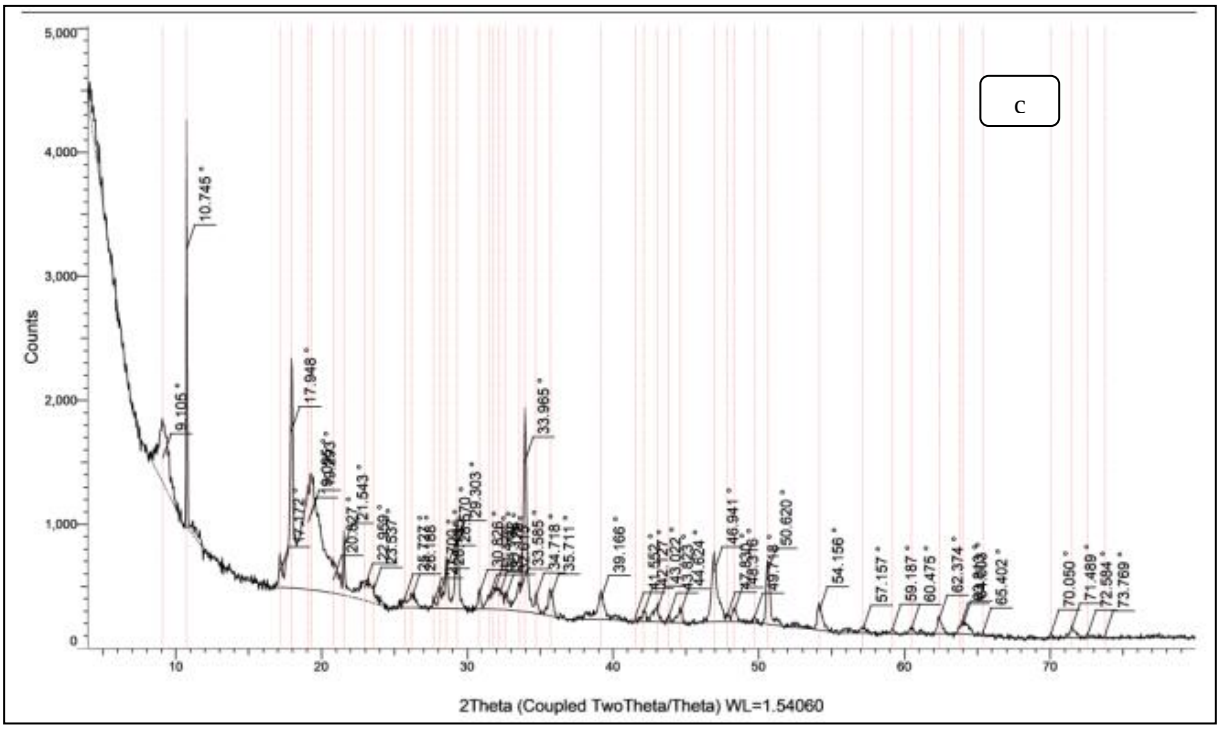
c
Counts
2Theta (Coupled TwoTheta/Theta) WL=1.54060
10.745 °
17.948 °
9.105 °
33.965 °
21.543 °
29.303 °
33.585 °
34.718 °
35.711 °
39.166 °
46.941 °
50.620 °
54.156 °
57.157 °
59.187 °
60.475 °
62.374 °
65.402 °
70.050 °
71.489 °
72.594 °
73.769 °

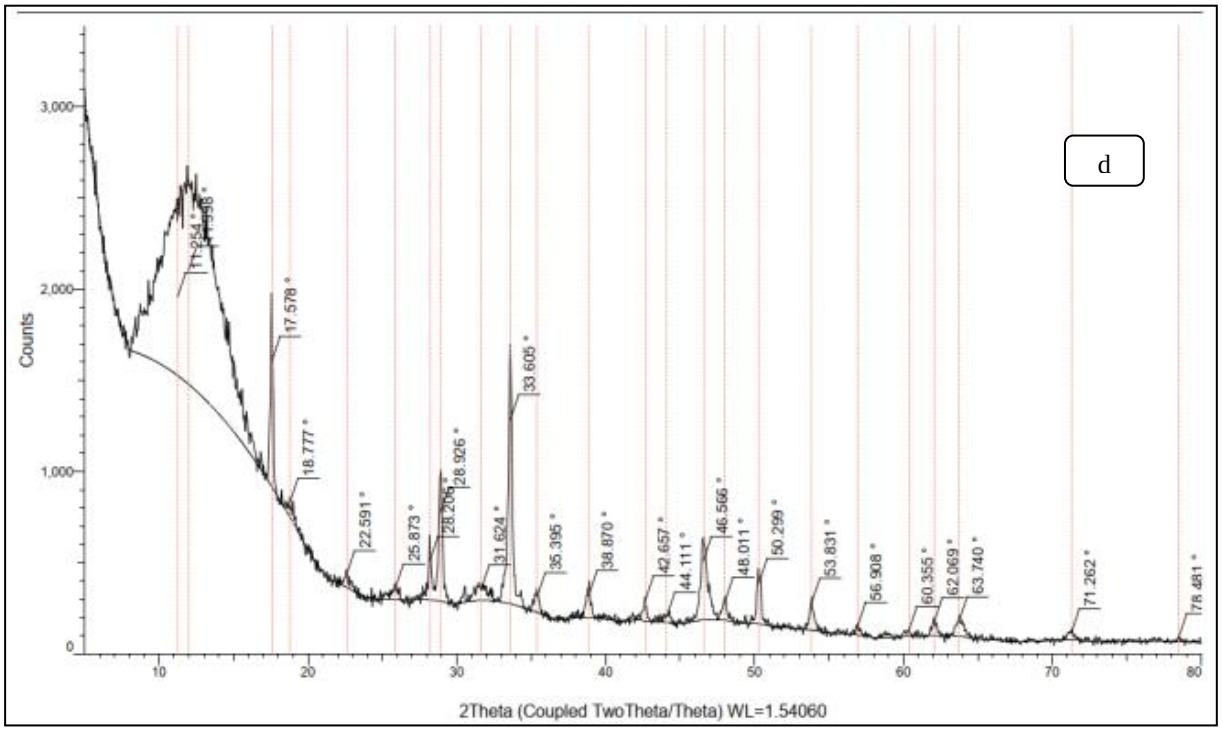
d
Counts
2Theta (Coupled TwoTheta/Theta) WL=1.54060
17.578 °
18.777 °
33.605 °
22.591 °
25.873 °
28.206 °
28.926 °
31.624 °
35.395 °
38.870 °
42.657 °
44.111 °
46.566 °
48.011 °
50.299 °
53.831 °
56.908 °
60.355 °
62.069 °
63.740 °
71.262 °
78.481 °

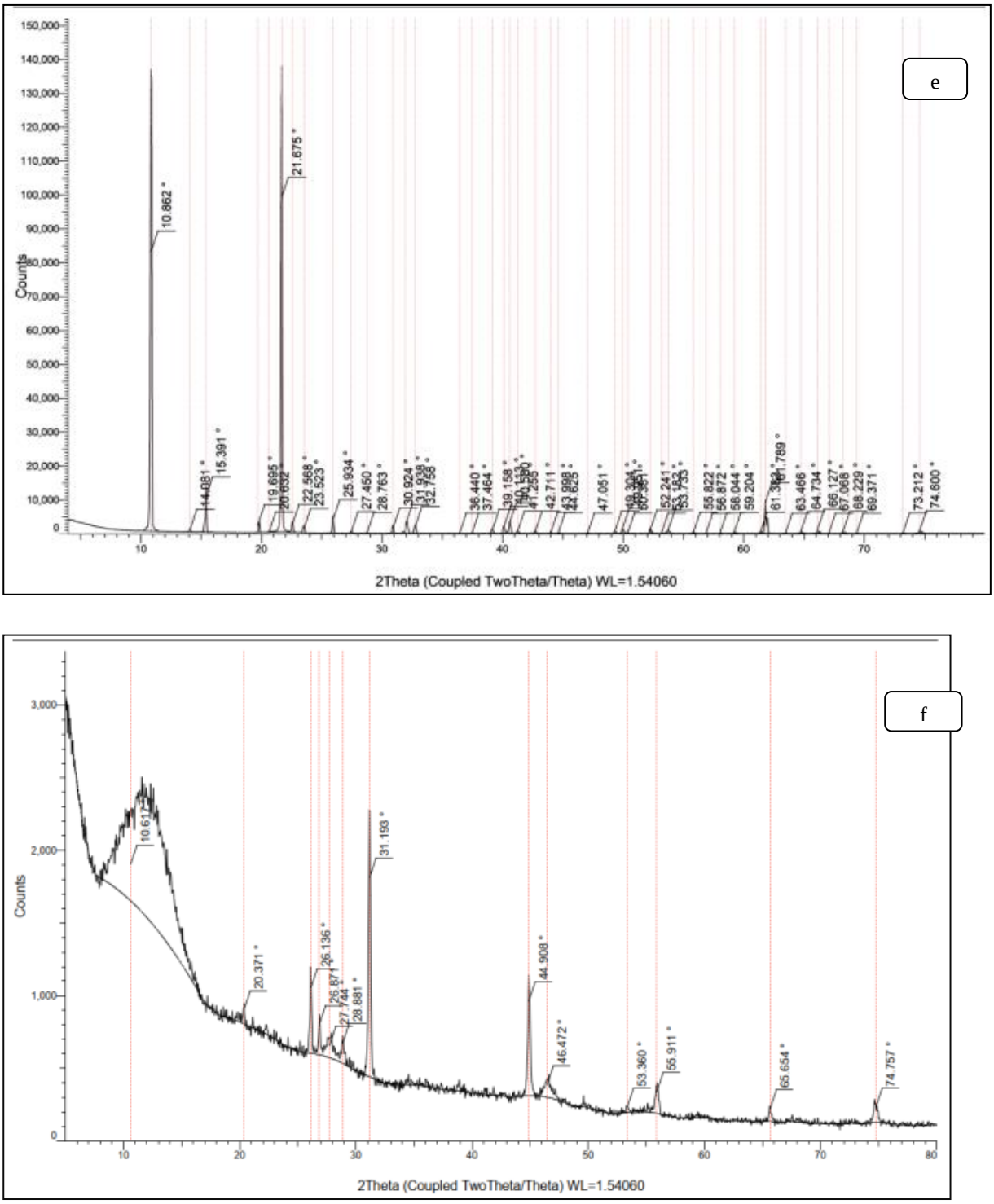

Fig. (2). X-ray diffraction patterns of **(a)** commercial chitosan, **(b)** commercial chitosan nanoparticles, **(c)** shrimp chitosan, **(d)** shrimp chitosan nanoparticles, **(e)** crab chitosan and **(f)** crab chitosan nanoparticles.

Shrimp chitosan XRD pattern showed the sharpest peak at 17.948° (1267.05 counts/s) and the highest peak at 10.745° (2237.91 counts/s). Shrimp chitosan nanoparticles XRD analysis maximum peaks at 31.193° (1372.72 counts/s).

The XRD studies of crab chitosan showed a sharper peak at 25.421° (4756.36 counts/s) and a maximum peak at 14.835° (8384.45 counts/s), while, crab chitosan nanoparticles revealed stronger peaks at 17.578° (687.760 counts/s) and a maximum reflection at 33.605° (1012.17 counts/s).
The XRD results of the chitosan samples showed the crystalline nature of obtained polymers. Similar results have been obtained in previous studies **[37-40].**

Energy Dispersive X-Ray spectroscopy (EDAX)

(EDS or EDAX) is an X-Ray non-destructive analysis used to identify the elemental composition of materials. Its principle based to convey an external X-ray stimulation on electrons of K bands within atoms, in order to one or more this electron leaves its orbit and will be replaced by an electron from L band, with emission of radiation energy kα, this last electron will be also replaced by an electron from M band with emission of Lα radiation energy. Furthermore, the electron of K band can be replaced directly by electron from M band with emission of Kβ radiation energy.

All of these energies radiation will be captured by the device's collector and processed in order to displays a spectrum with different peaks. Each peak corresponds to a unique chemical element with its atomic and weight concentration **[41].**
All EDX spectrum chromatograms of commercial, crab, shrimp chitosan and their nanoparticles are presented in **(fig. 3a-f and fig. 4).** The obtained results recorded in Table 3, and plotted in Figure 4 in order to compare easily the elemental weight and atomic concentration percentages in each chitosan samples.

The obtained results indicated that all samples contained carbon C, nitrogen N and oxygen O with a different intensities related to their concentration in each chitosan and chitosan nanoparticles samples. While, phosphorus P, calcium Ca potassium K, sodium Na, Magnesium Mg, silicate Si and copper Cu were found in shrimp and crab chitosan and their nanoparticles. This result proves the incapacity of diluted acid to remove all minerals from the shrimp and crab shells, contrary to concentrated acids can maybe leave just a few minerals traces **[42].**

Scanning Electron Microscopy (SEM)

The morphological characteristics of chitosan (commercial, shrimp, crab) and its nanoparticles were evaluated by scanning electron microscopy **(fig. 5a-f)**.

The SEM micrographs showed that, there are obvious difference in the roughness and surface morphology among the different types of chitosan and its nanoparticles types and showed a relatively smooth top surface and fibrous structures. Commercial chitosan represents a smooth surface morphology and fibrous structures with pores at 300 µm, while, commercial nanoparticles shows a combination of rough and smooth layers and a combination of fibers and pores at 40 µm. Additionally, shrimp chitosan presents a very smooth surface at 20 µm, while shrimp nanoparticles reveals a porous and fibrous surface morphology at 20 µm. Crab chitosan presents a hard and rough surface morphology at 40 µm, while crab nanoparticles had fibrous structures at 40 µm. This results are in agreement with studies reported by **[30, 33, 38, 43].**

Table (3). Elementary EDAX analysis for commercial, shrimp and crab chitosan and its nanoparticles.

Element	Weight %	Atomic %	Net Int.	Error %
Commercial chitosan				
C K	29.02	34.62	41.25	9.02
N K	14.41	14.74	7.13	23.31
O K	56.57	50.65	70.03	11.79
Commercial Chitosan nanoparticles				
C K	38.37	44.6	75.07	7.69
N K	12.96	12.92	6.44	24.05
O K	48.67	42.47	67.63	12.08
Shrimp chitosan				
C K	46.41	54.16	188.53	6.57
N K	6.16	6.16	4.77	29.96
O K	43.71	38.3	114.9	11.43
Mg K	0.26	0.15	3.67	65.23
Si K	0.11	0.05	2.3	65.23
Ca K	3.36	1.17	43.7	12
Shrimp chitosan nanoparticles				
C K	16.5	27.14	26.45	11.57
N K	0.75	1.06	0.26	99.99
O K	39.41	48.66	45.43	13.19
Na K	3.81	3.28	14.65	18.46
Mg K	0.07	0.05	0.47	83.87
P K	2.43	1.55	25.54	13.48
K K	1.52	0.77	15.62	17.78
Ca K	35.5	17.49	266.39	2.78
Crab chitosan				
C K	35.86	46.84	47.17	9.93
N K	3.45	3.86	1.28	78.18
O K	41.76	40.95	54.31	12.38
NaK	4.53	3.09	14.28	16.95
MgK	0.34	0.22	1.93	70.06
P K	1.63	0.82	13.24	16.04
K K	0.53	0.21	3.84	60.4
Ca K	7.36	2.88	43.76	7.75
Cu K	4.54	1.12	7.39	23.77
Crab chitosan nanoparticles				
C K	35.61	44.05	104.09	8.76
N K	6.84	7.26	6.31	26.94
O K	44.44	41.28	134.36	10.89
Na K	7.31	4.73	55.96	11.03
Mg K	1.33	0.81	16.94	17.03
Si K	1.41	0.74	27.45	12.13
Ca K	3.07	1.14	39.34	13.24

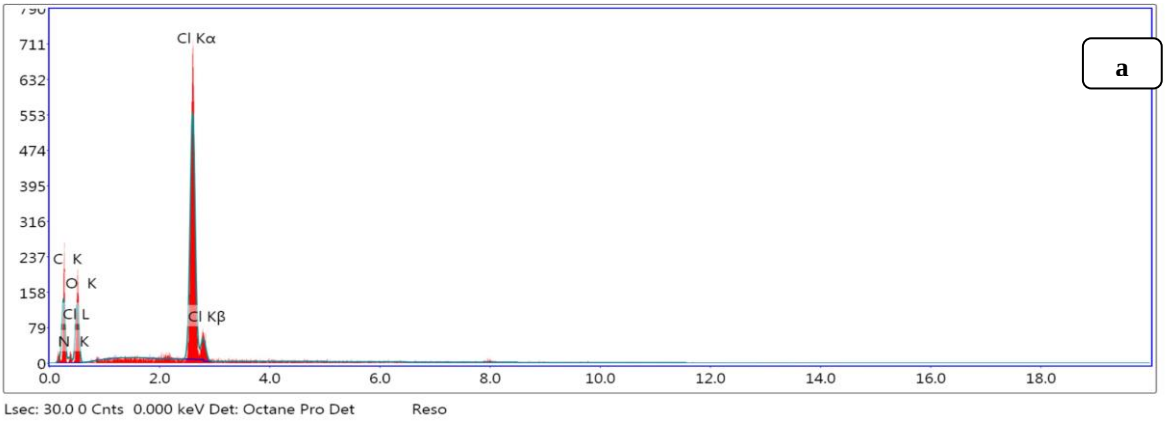
a
Cl Kα
C K
O K
Cl L
N K
Cl Kβ
0.0 2.0 4.0 6.0 8.0 10.0 12.0 14.0 16.0 18.0
Lsec: 30.0 0 Cnts 0.000 keV Det: Octane Pro Det Reso

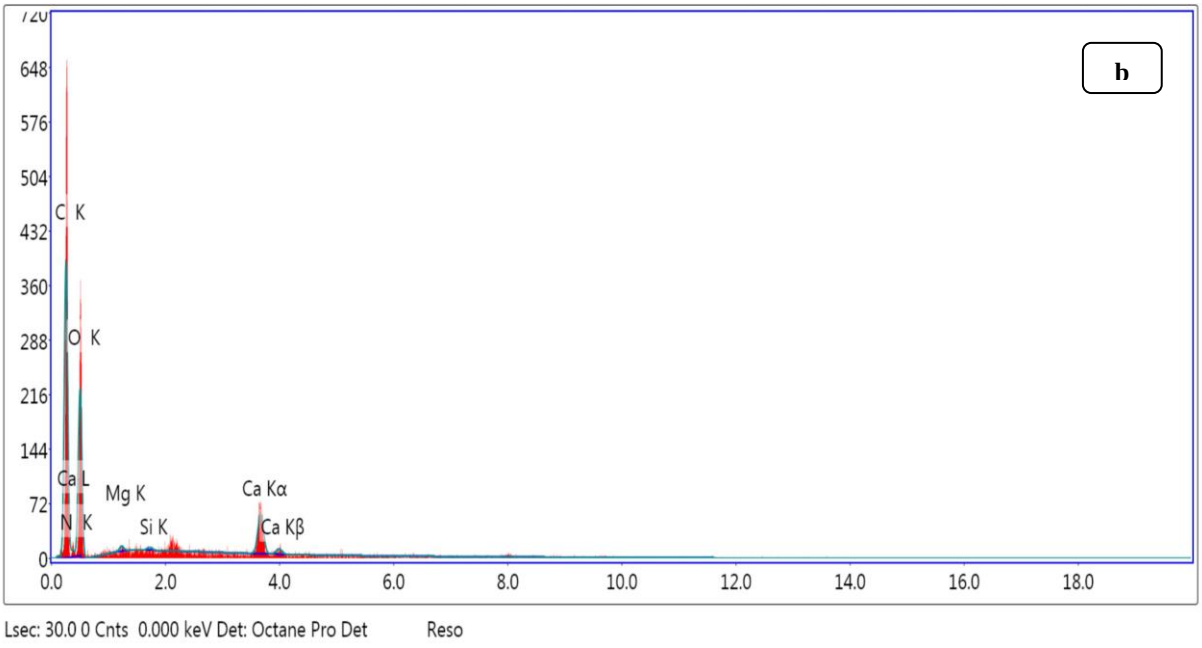
b
C K
O K
Ca L
N K
Mg K
Si K
Ca Kα
Ca Kβ
0.0 2.0 4.0 6.0 8.0 10.0 12.0 14.0 16.0 18.0
Lsec: 30.0 0 Cnts 0.000 keV Det: Octane Pro Det Reso

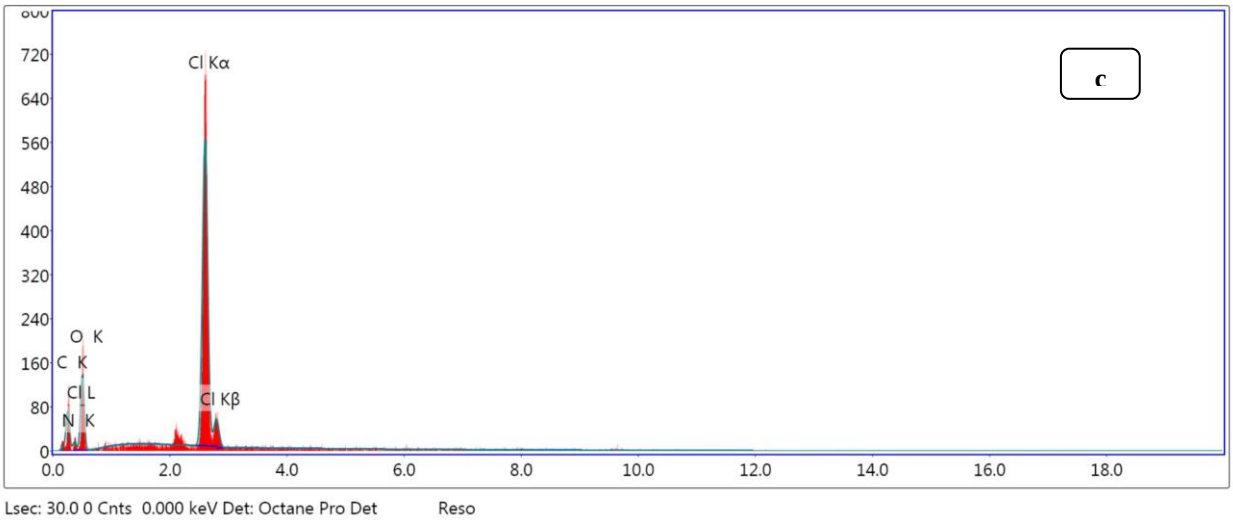
c
Cl Kα
O K
C K
Cl L
N K
Cl Kβ
0.0 2.0 4.0 6.0 8.0 10.0 12.0 14.0 16.0 18.0
Lsec: 30.0 0 Cnts 0.000 keV Det: Octane Pro Det Reso

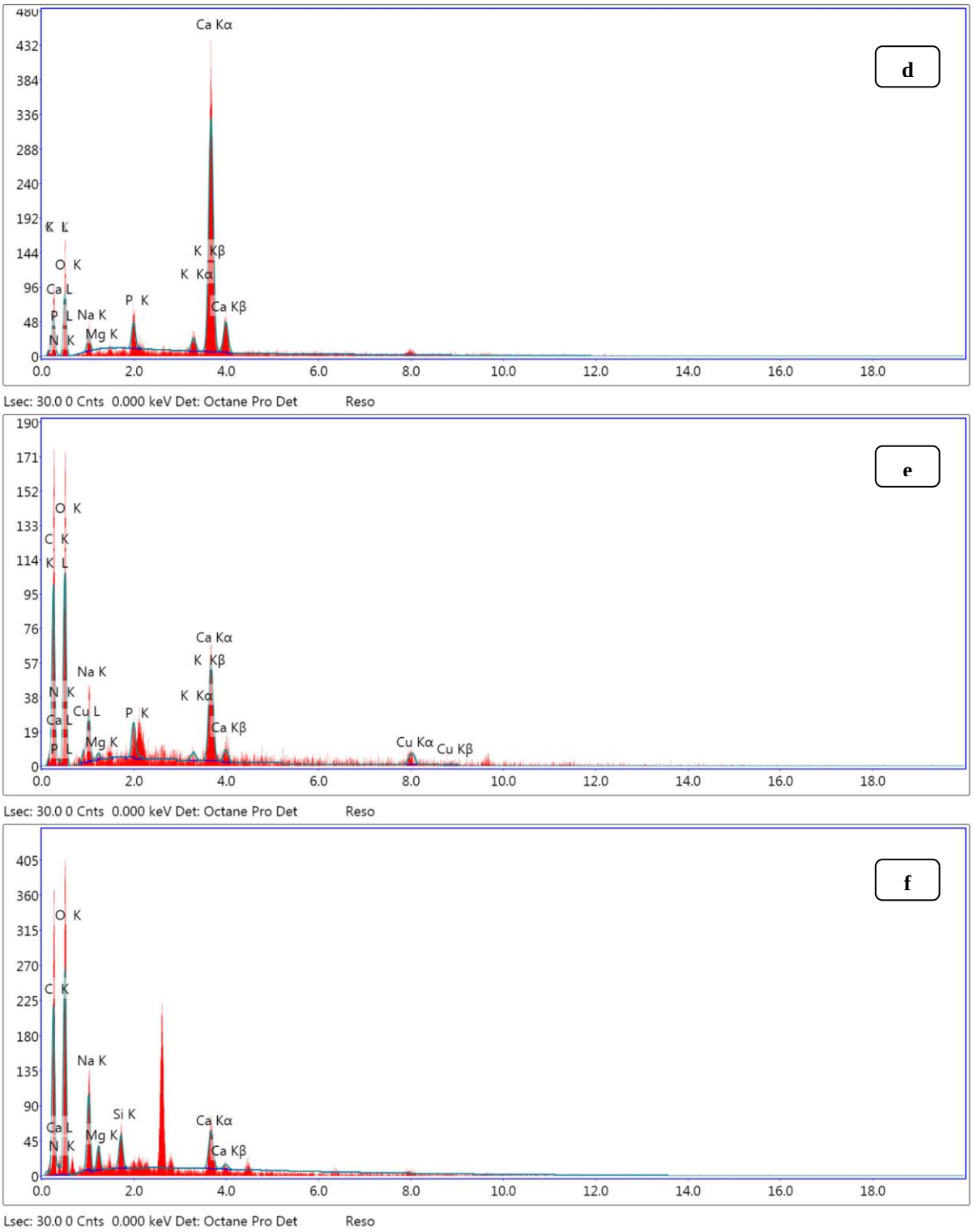

Fig. (3). EDAX of (a) commercial chitosan, (b) commercial chitosan nanoparticles, (c) shrimp chitosan, (d) shrimp chitosan nanoparticles, (e) crab chitosan and (f) crab chitosan nanoparticles.

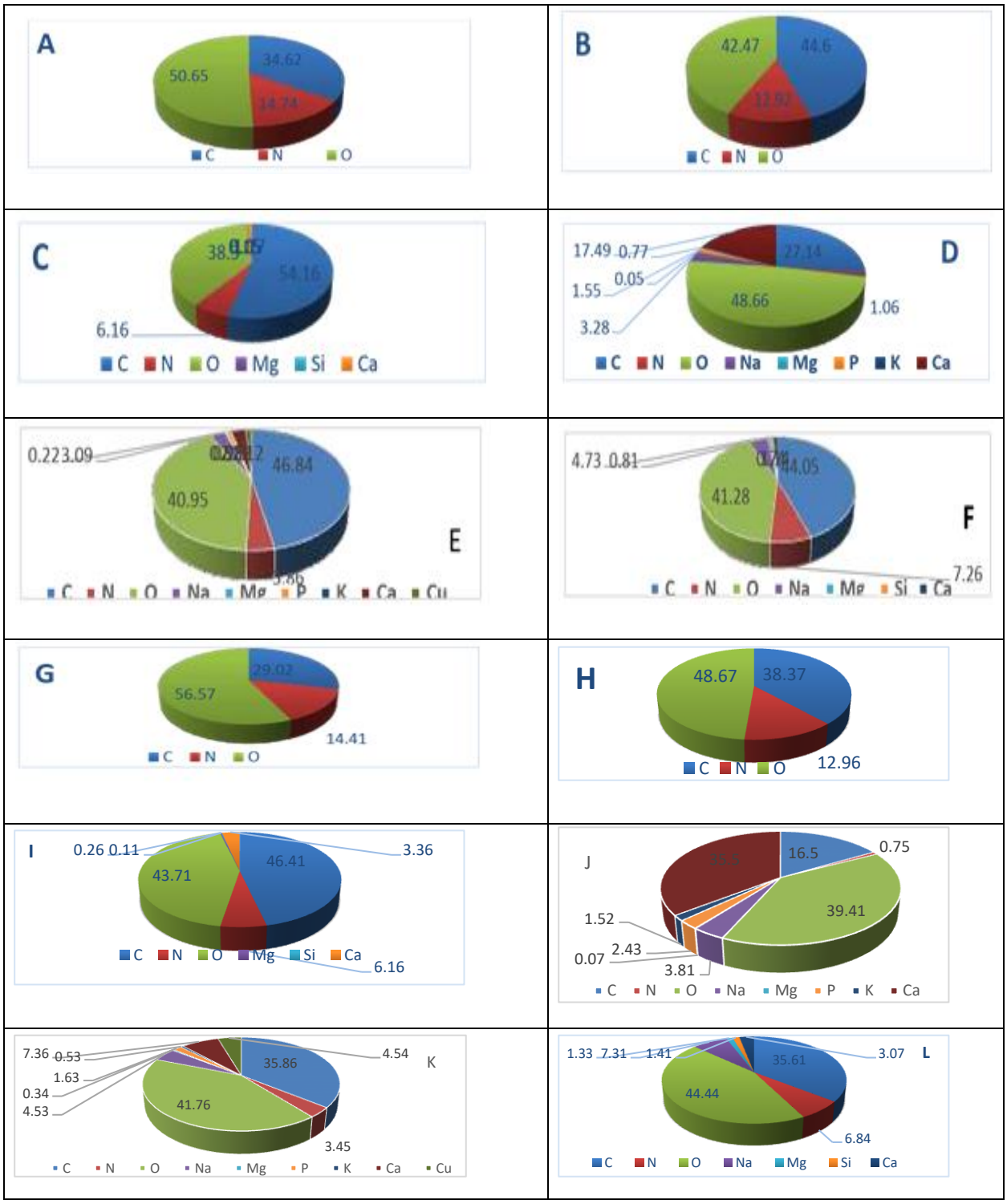

Fig. (4). Represent the percentage of the atomic element of (a) commercial chitosan, (b) commercial chitosan nanoparticles, (c) shrimp chitosan, (d) shrimp chitosan nanoparticles, (e) crab chitosan and (f) crab chitosan nanoparticles, while, Elementals weight concentrations (g) commercial chitosan, (h) commercial chitosan nanoparticles, (I) shrimp chitosan, (J) shrimp chitosan nanoparticles, (K) crab chitosan and (L) crab chitosan nanoparticles.

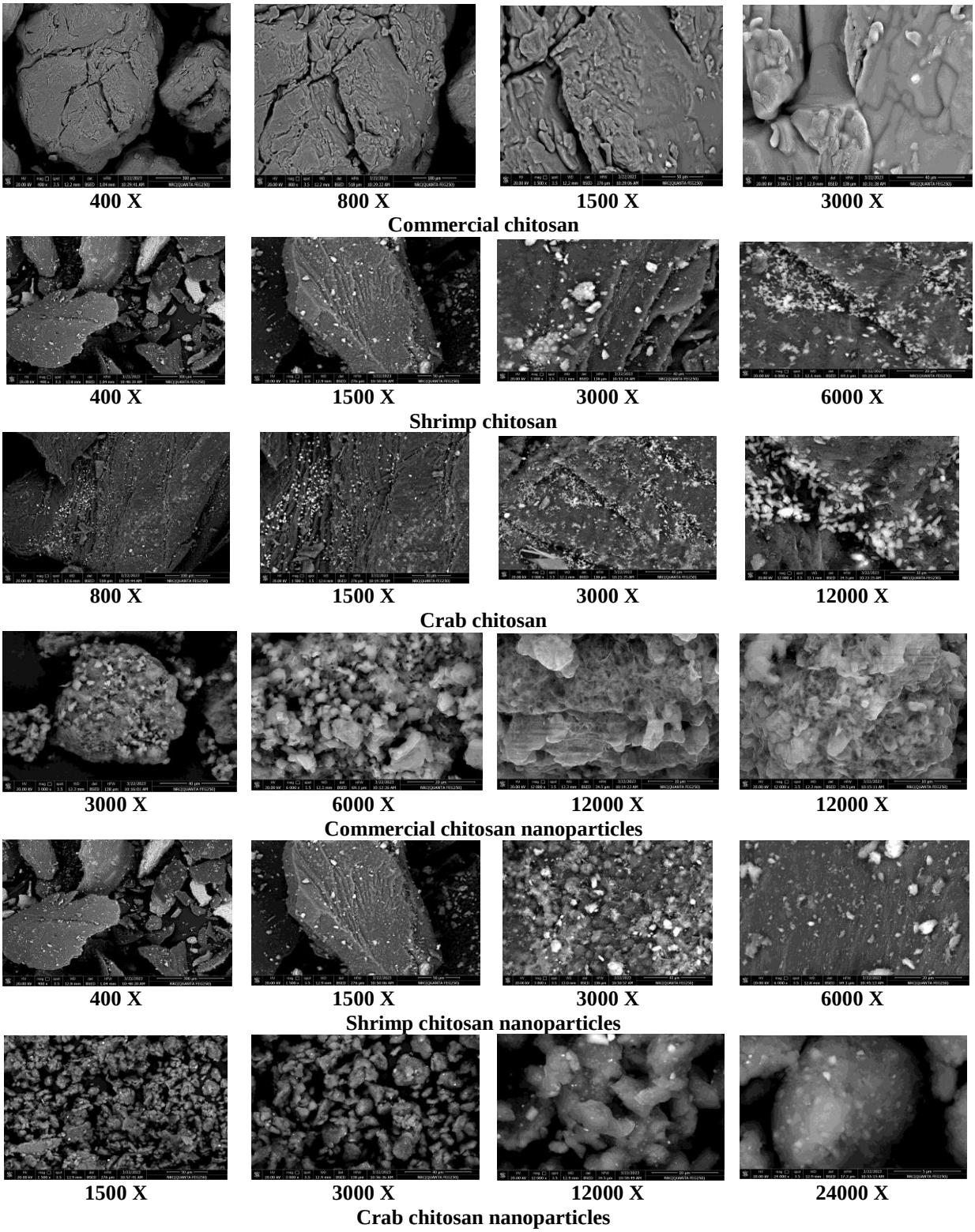

Fig. (5). SEM of chitosan samples and their nanoparticles size at different magnificent levels.

4. Conclusion

Chitosan and its prepared nano-particle of shrimp and crab have a good physiochemical and functional properties when compared with the commercial chitosan.

5. Conflicts of interest

The authors declare that there are no conflicts of interest.

6. Acknowledgements

This study was funded according to a scientific cooperation protocol between National Institute of Oceanography & Fisheries and National Research Centre. Therefore, their kind support is greatly appreciated.

6. References

[1] Vicente F.A., Ventura S.P.M., Passos H., Dias A.C.R.V., Torres-Acosta M.A., Novak U., Likozar B. Crustacean waste biorefinery as a sustainable cost-effective business Model. Chem. Eng. J., 2022, 442, 135937.

[2] Salah R., Michaud P., F. Mati, et al. Anticancer activity of chemically prepared shrimp low molecular weight chitin evaluation with the human monocyte leukaemia cell line, THP-1, Int. J. Biol. Macromol., 2013, 52, 333–339.

[3] Bouhenna M., Salah R., Bakour R., *et al*. Effects of chitin and its derivatives on human cancer cells lines, Environ. Sci. Pollut. Control Ser., 2015, 22 (20) 15579–15586.

[4] Benhabiles M.S., Abdi N., Drouiche N., et al. Protein recovery by ultrafiltration during isolation of chitin from shrimp shells *Parapenaeus longirostris*, Food Hydrocolloids, 2013, 32 (1) 28–34.

[5] Darmon S.E., Rudall K.M. Infra-red and X-ray studies of chitin, Discuss. Faraday Soc., 1950, 9, 251–260.

[6] Jack G. Winterowd, Paul A. Sandford. Chitin and chitosan, Food Science and Technology-New York-Marcel Dekker, 1995, 441.

[7] Hoppe-seyler F. Ueber chitin und cellulose, Ber. Dtsch. Chem. Ges., 1894, 27 (3) 3329–3331.

[8] Qi L., Xu Z., Jiang X., Hu C., Zou X. Preparation and antibacterial activity of chitosan nanoparticles. Carbohydr. Res., 2004, 339 (16): 2693-2700.

[9] Ali, S. W., Joshi, M., & Rajendran, S. Synthesis and characterization of chitosan nanoparticles with enhanced antimicrobial activity. International Journal of Nanoscience, 2011, 10 (04n05): 979–984.

[10] Saharan V., A. Mehrotra, R. Khatik, P. Rawal, S.S. Sharma, A. P. Synthesis of chitosan based nanoparticles and their in vitro evaluation against phytopathogenic fungi, Int. J. Biol. Macromol., 2013, 62: 677–683.

[11] Sathiyabama M., and Parthasarathy R. Biological preparation of chitosan nanoparticles and it's in vitro antifungal efficacy against some phytopathogenic fungi. Carbohydr. Polym., 2016, 151, 321–325.

[12] Toan N.V. Production of chitin and chitosan from partially autolyzed shrimp shell materials. The Open Biomaterials Journal, 2009, 1: 21-24.

[13] Dutta P.K., Dutta J., Tripathi V.S. Chitin and chitosan: chemistry, property and application. J. Sci. Ind. Res., 63, 20-31 (2004).

[14] Joni, I. M., Panatarani C. and Maulana. D. W. Dispersion of fine phosphor particles by newly developed beads mill, in The 2ndPadjadjaran International Physics Symposium 2015 (PIPS-2015): Materials Functionalization and Energy Conservations, AIP Conf. Proc. 1712, edited by I M. Joni et al. (American Institute of Physics, Melville, N.Y., 2016, 050019-1–050019-6.

[15] Inkyo, M., Tahara T., Iwaki T., Iskandar F., C. Hogen J., Okuyama K. and Colloid J. Experimental investigation of nanoparticles dispersion by beads milling with centrifugal bead separation, J. Colloid Interf., 2006, Sci. 304, 535–540.

[16] Ibrahim, A.I., Ebeid H.M., Kishk Y.F.M., Abdel Fattah A.A. and Mahmoud K.F. Effect of grinding and particle size on some physical and rheological properties of chitosan. Arab Universities Journal of Agricultural Sciences, Ain Shams Univ., Cairo, Egypt, 2019, 27(2): 1513-1527.

[17] AOAC, Official Methods of Analysis of the Association of Official Analytical Chemistry (AOAC) International, 18th ed., Gaithersburg, Maryland, USA (2007).

[18] Mohanasrinivasan V., Mishra M., Paliwal J., Singh S., Selvarajan E., Suganthi V., et al., Studies on heavy metal removal efficiency and antibacterial activity of chitosan prepared from shrimp shell waste. Biotech., 2014, 4: 167-75.

[19] Wang J.C., Kinsella J.E. Functional properties of novel proteins: Alfalfa leaf protein. J. Food Sci., 1976, 41, 286-292.

[20] Struszczyk H. Microcrystalline chitosan. Preparation and properties of microcrystalline chitosan. J. Appl. Polym. Sci., 1987, 33: 177-189.

[21] Luo Q., Wang Y., Han Q., Ji L., Zhang, H., Fei, Z., Wang Y. Comparison of the Physicochemical, Rheological, and Morphologic Properties of Chitosan from Four Insects. Carbohydr. Polym., 2019, 209: 266–275.

[22] Ocloo F.C.K., Quayson E.T., Adu-Gyamfi A., Quarcoo E.A., Asare D., Serfor-Armah Y., Woode B.K. Physicochemical and Functional Characteristics of Radiation-Processed Shrimp Chitosan. Radiat. Phys. Chem., 2011, 80: 837–841.

[23] Muley A.B., Chaudhari S.A., Mulchandani K.H. and Singhal R.S. Extraction and characterization of chitosan from prawn shell waste and its conjugation with cutinase for enhanced thermo-stability. Int. J. Biol. Macromol., 2018, 111: 1047–1058.

[24] Baron R.D., Pérez L.L., Salcedo J.M., Córdoba L.P. and Sobral P.J.d.A. Production and Characterization of Films Based on Blends of Chitosan from Blue Crab (*Callinectes sapidus*) Waste and Pectin from Orange (*Citrus sinensis* Osbeck) Peel. Int. J. Biol. Macromol., 2017, 98, 676–683.

[25] Kumari S., Kumar Annamareddy S.H., Abanti S. and Kumar Rath P. Physicochemical properties and characterization of chitosan synthesized from fish scales, crab and shrimp shells. Int. J. Biol. Macromol., 2017, 104: 1697–1705.

[26] Hossain M. and Iqbal, A. Production and characterization of chitosan from shrimp waste. J. Bangladesh Agric. Univ., 2014, 12: 153–160.

[27] Chien, R.C., Yen, M.T. and Mau J.L. Antimicrobial and antitumor activities of chitosan from shiitake stipes, compared to commercial chitosan from crab shells. Carbohydr. Polym., 2016, 138: 259–264.

[28] Bhardwaj S., Bhardwaj N.K. and Negi, Y.S. Effect of degree of deacetylation of chitosan on its performance as surface application chemical for paper-based packaging. Cellulose, 2020, 27, 5337–5352.

[29] Pakizeh M., Moradi A., Ghassemi T. Chemical extraction and modification of chitin and chitosan from shrimp shells. Eur. Polym. J., 2021, 159: 110709.

[30] Ghannam H.E., Talab A.S., Dolganova N.V., Hussein A.M.S. and Abdelmaguid N.M. Characterization of chitosan extracted from different crustacean shell wastes. Journal of Applied Science, 2016, 16: 454-461.

[31] Olaosebikan, A.O., Kehinde, O.A., Tolulase, O.A. and Victor, E.B. Extraction and Characterization of Chitin and chitosan from *Callinectes amnicola* and *Penaeus notialis* shell wastes. J. Chem. Eng. Mater. Sci., 2021, 12: 1–30.

[32] Yarnpakdee, S., Kaewprachu, P., Jaisan, C., Senphan, T., Nagarajan, M. and Wangtueai, S. Extraction and physico–chemical characterization of chitosan from mantis shrimp (*Oratosquilla nepa*) shell and the development of bio-composite film with agarose. Polymers, 2022, 14: 3983.

[33] El-araby A., El Ghadraoui L. and Errachidi F. Physicochemical properties and functional characteristics of ecologically extracted shrimp chitosans with different organic acids during demineralization step. Molecules, 2022a, 27: 8285.

[34] Rakkhumkaew, N. and Pengsuk, C. Chitosan and chitooligosaccharides from shrimp shell waste: characterization, antimicrobial and shelf life extension in bread. Food Sci. Biotechnol., 2018, 27: 1201-1208.

[35] Varma, R. and Vasudevan, S. Extraction, characterization, and antimicrobial activity of chitosan from horse mussel *Modiolus Modiolus*. ACS Omega 5, 2020, 20224–20230.

[36] Panda P.K., Dash P., Chang Y.H. and Yang, J.M. Improvement of chitosan water solubility by fumaric acid modification. Mater. Lett., 2022, 316, 132046.

[37] Rasti H., Parivar K., Baharara J., Iranshahi M. and Namvar F. Chitin from the mollusc chiton: extraction, characterization and chitosan preparation. Iran. J. Pharm. Res., 2017, 16: 366.

[38] Ibitoye E.B., Lokman I.H., Hezmee M.N.M., Goh Y.M., Zuki A.B.Z. and Jimoh A.A. Extraction and physicochemical characterization of chitin and chitosan isolated from house cricket. Biomed. Mater., 2018, 13, 025009.

[39] Kuyyogsuy A. Preparation and characterization of chitosan obtained from pacific white shrimp shells and its in vitro antifungal activity. Asian J. Chem., 2020, 32, 2515–2519.

[40] El-araby A., El Ghadraoui L. and Errachidi F. Usage of biological chitosan against the contamination of post-harvest treatment of strawberries by *Aspergillus niger*. Front. Sustain. Food Syst., 2022b, 6, 881434.

[41] Lovejoy T.C., Ramasse Q.M., Falke M., et al., Single atom identification by energy dispersive x-ray spectroscopy, Appl. Phys. Lett., 2012, 100 (15): 154101.

[42] Eddya M., Tbib B. and EL-Hami Kh. A comparison of chitosan properties after extraction from shrimp shells by diluted and concentrated acids. Heliyon, 2020, 6, e03486.

[43] Tolesa L.D., Gupta B.S. and Lee M.J. Chitin and chitosan production from shrimp shells using ammonium-based ionic liquids. Int. J. Biol. Macromol., 2019, 130: 818–826.